ACS Macro Letters

Letter

pubs.acs.org/macroletters

Polymeric Micelles with Mesoporous Cores

Yue Zhang,[†] Chuanzhuang Zhao,[†] Li Liu,*[,‡] and Hanying Zhao*[,†]

[†]Department of Chemistry and [‡]Institute of Polymer Chemistry, Key Laboratory of Functional Polymer Materials, Ministry of Education, Nankai University, Tianjin 300071, China

Supporting Information

ABSTRACT: Mesoporous polymer nanoparticles containing pores with sizes ranging from 2 to 50 nm are attractive for wide applications, such as catalysis, drug delivery, and separations. On the basis of nanometer-sized phase separation and cleavage reaction in the micellar cores, polymeric micelles with mesoporous cores are prepared in this research. A triblock terpolymer, consisting of one hydrophilic block and two mutually incompatible hydrophobic blocks covalently connected by a redox-responsive disulfide linkage, self-assembles into multicompartment micelles, a type of micelle with subdivided hydrophobic cores, in aqueous solution. Due to the incompatibility, the two hydrophobic blocks have nanometer-sized phase separation in the micellar cores, one in the discontinuous phase and the other in the continuous phase. Upon cleavage of the disulfide linkage, the discontinuous phase is dissolved in a selective solvent, and micelles with mesoporous cores are obtained. The average pore size is around 3 nm. Functionalization of the mesopores with functional compounds and inorganic nanoparticles renders these micelles suited for wide applications.

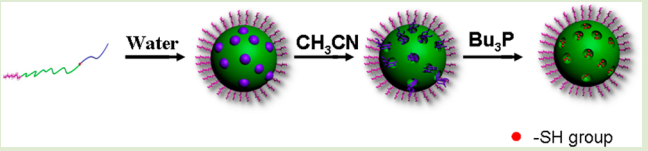

With the rapid development of nanoscience, many well-defined materials at the nanometer-length scale have been produced. These materials include individual atoms or clusters, as well as block copolymers which are able to self-assemble into advanced structures by the bottom-up approach. Block copolymers, which are able to self-assemble into different patterns on solid surfaces or nanostructures in solutions, provide an opportunity to fabricate complex and multifunctional nanostructures.[1,2] Like small molecule amphiphiles, amphiphilic linear block copolymers can make spontaneous arrangements into aggregates or micelles of various morphologies in aqueous solutions, such as spheres, cylinders, vesicles,[3] bowls,[4] discs,[5] helices,[6] and toroids.[7] These structures have found wide applications in the development of new nanotechnologies, including nanoparticle synthesis,[8] nanolithography,[9] and drug delivery.[10] The morphology of the free-energy driven aggregates can be tuned by a series of control variables, including chemical composition, block length, polymer architecture, and variation of solution conditions. Among the aggregates, spherical micelles are well studied and considered to be promising in practical applications. Continuous efforts have been made to improve the structure and functionality of the spherical micelles, and core cross-linked, shell cross-linked, interface cross-linked, and functional group decorated micelles were obtained.[11−14]

As pointed out by Ringsdorf in 1988 that "polymer science is able to contribute to the simulation of cellular process",[15] the self-assemblies of block copolymers with specific structures are used to mimic the biological structures. Serum albumin is a transport protein in the blood bearing several different specific binding sites for different poorly water-soluble compounds, such as fatty acids, vitamins, hormones, and drugs. The simplified biological analogy to the transport protein resulted in the topic of multicompartment micelles.[16−18] Multicompartment micelles are self-assembled by triblock terpolymers with one solvophilic block and two mutually immiscible solvophobic blocks. The two solvophobic blocks readily undergo nanometer-sized phase separation within the solvophobic cores affording the discrete subdomains, which can facilitate the concurrent storage and therapeutic delivery of multiple incompatible payloads.[17] Utilizing starlike triblock terpolymers by Lodge, Hillmyer, and co-workers[19] and linear triblock terpolymers by Laschewsky and co-workers,[20] multicompartment micelles were prepared. The multicompartment micelles hold great promise for "smart" drug or gene delivery applications.

Another type of interesting structure, which can be used to mimic biological structures especially bone structures, is mesoporous structure. Mesoporous structure has drawn a lot of attention for its controllable pore surface chemistry, tunable pore size, large specific surface area, and low bulk density.[21] Mesoporous structures, especially functional voids or channels in the solid matrix, can be used to mimic the transport process of biomolecules through a biological membrane. Mesoporous materials have found wide applications in catalysis, drug delivery, and imaging.[22] For example, ordered mesoporous silica particles show potentials to boost the in vitro and in vivo dissolution of poorly water-soluble drugs.[23] In this paper, we report the preparation and functionalization of polymeric micelles with mesoporous cores. A triblock terpolymer, consisting of one hydrophilic block and two mutually incompatible hydrophobic blocks, self-assembles into multi-

Received: June 4, 2013
Accepted: September 17, 2013
Published: September 20, 2013

compartment micelles in aqueous solution. Due to the incompatibility, the two hydrophobic blocks have nanometer-sized phase separation in the micellar cores. Upon cleavage of the disulfide bonds at the junction points between the two hydrophobic blocks, the discontinuous phase is dissolved in a selective solvent, and micelles with mesoporous cores are prepared.

The polymer used in this research is a linear triblock terpolymer of poly(ε-caprolactone) (PCL), polystyrene (PS), and poly(oligo(ethylene glycol) monomethyl ether methacrylate) (POEGMA) (Figure 1a), where PCL and PS are

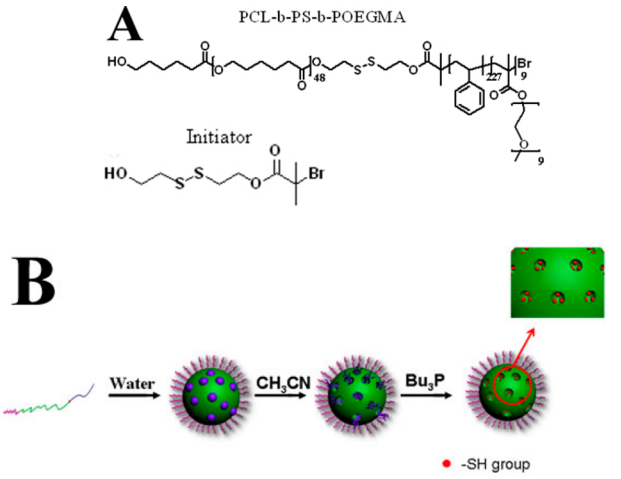

Figure 1. (A) Molecular structures of triblock terpolymer, PCL-*b*-PS-b-POEGMA, and initiator used in the synthesis of the polymer. (B) Schematic depiction of the preparation of micelles with mesoporous cores. In aqueous solution, the PCL-*b*-PS-*b*-POEGMA triblock terpolymer self-assembles into micelles with POEGMA shells and PCL/PS cores. In the hydrophobic micellar core, PCL forms discontinuous phases in the PS matrix, and after PCL etching, micelles with porous cores are produced.

hydrophobic and POEGMA is hydrophilic. One feature of the triblock terpolymer is that there is a redox-responsive disulfide group at the junction point between the PCL and PS block. In the synthesis of the triblock terpolymer, 2-bromo-2-methyl-propionic acid 2-(2-hydroxy-ethyldisulfanyl)-ethyl ester (Figure 1a) was used as an initiator [see Supporting Information for ^{1}H NMR spectrum (Figure S1)]. In an initiator molecule, there is one hydroxyl group and one bromo group at two molecular ends and a disulfide group at the midpoint. Initiated by the terminal hydroxyl group, PCL was synthesized by ring-opening polymerization (ROP) of CL; initiated by the terminal bromo group, PS-*b*-POEGMA diblocks were synthesized by two-step atom transfer radical polymerization (ATRP). OEGMA used in this research is a methacrylate-based macromonomer with pendant oligo(ethylene glycol) (EG) chains (M = 475 g/mol, with nine pendent EG units). On the basis of ^{1}H NMR results, the average repeating unit numbers of PCL, PS, and POEGMA are 49, 227, and 9 (Figures S2, S3, and S4 in the Supporting Information). The apparent number-average molecular weight and the dispersity of the triblock terpolymer, estimated by size exclusion chromatography (SEC), are 33.5 K and 1.20 (Figure S5, Supporting Information).

In aqueous solution, the triblock terpolymer self-assembles into micellar structure with a hydrophobic core and a hydrophilic corona. PCL and PS are characterized by a large Flory–Huggins interaction parameter;[24] the two hydrophobic blocks segregate into distinct domains in the core; and the hydrophilic POEGMA blocks form the corona to stabilize the structure. In the triblock terpolymer, the PCL block is shorter than PS, and the volume percentage of PCL in a micellar core is about 17.7%, much lower than PS; so, PCL blocks form the discontinuous phase, and PS blocks form the continuous phase in a micellar core. The two phases are covalently connected by disulfide bonds. After freeze-drying, the micelles were redispersed into acetonitrile, a good solvent for POEGMA and PCL but a precipitant for PS. PCL blocks are solvated, and the core structure is held together by the continuous PS phase. Upon addition of tri-*n*-butylphosphine (Bu_3P) into the solution, disulfide bonds are cleaved, and PCL blocks go into the acetonitrile phase leaving void structures inside the micellar cores. The cleavage of the disulfide bonds not only creates the void structures inside the micellar cores but also offers the advantage of the functionalization of the pores with thiol groups. A schematic of the overall process is given in Figure 1b.

The thiol group has many applications in chemistry and materials science. For example, it can undergo both the radical-mediated and base/nucleophile-initiated thiol–ene reactions,[25] and it has a very high affinity to the surface of gold nanoparticles (AuNPs), which can be used in the surface modification of AuNPs.[26] In this research, by taking advantage of the thiol groups on the walls of the pores, pyrenyl groups, fluorescein *O*-methacrylate (FMA) functional groups, as well as AuNPs were introduced into the pores inside the micellar cores, and functional self-assembled structures were fabricated.

The self-assembly of the triblock terpolymer, PCL_{49}-b-PS_{227}-b-$POEGMA_9$, in an aqueous solution prepared by introducing water to the polymer solution in THF (a good solvent for all the three blocks), and followed by subsequent dialysis against water, results in the nanostructures displayed in Figure 2a and b. Spherical micelles containing internal phase-segregated domains in the cores are observed. The polymeric micelles on carbon-coated copper grids were stained in RuO_4 atmosphere for 45 min; therefore, the continuous dark domains represent PS phases in the cores, and the light domains represent PCL phases. The sizes of the PCL phases are in the range from 3 to 4 nm. Thus, on average there are four PCL chains in a PCL domain.[27] TEM analysis was also conducted on a sample drop deposited on a copper grid coated with a layer of graphene oxide (Figure 2c).[28] Nanosized-phase separation in the cores of micelles can be observed. The dynamic light scattering (DLS) result confirmed that uniform nanosized aggregates were obtained (PDI = 0.072, cumulant analysis), with an average hydrodynamic diameter (D_h) of 86 nm (Figure 2c). The nanosized phase separation structure in the micellar cores provides a perfect template for the preparation of the mesoporous core.

After freeze-drying, polymeric micelles were redispersed into acetonitrile solution. DLS result indicates that uniform nanostructures (D_h = 127, PDI = 0.028, Figure S6, Supporting Information) were obtained in acetonitrile. Because acetonitrile is a good solvent for PCL and POEGMA, and a precipitant for PS, we propose that in an individual nanostructure there exists a core composed of collapsed PS blocks and solvated PCL blocks and a POEGMA corona. It is worth noting that due to the solvation of the PCL blocks the average size of the aggregates in acetonitrile is bigger than the nanostructures prepared in aqueous solution. Transmission electron microscopy (TEM) results reveal that spherical assemblies with

dx.doi.org/10.1021/mz400286d | *ACS Macro Lett.* 2013, 2, 891–895

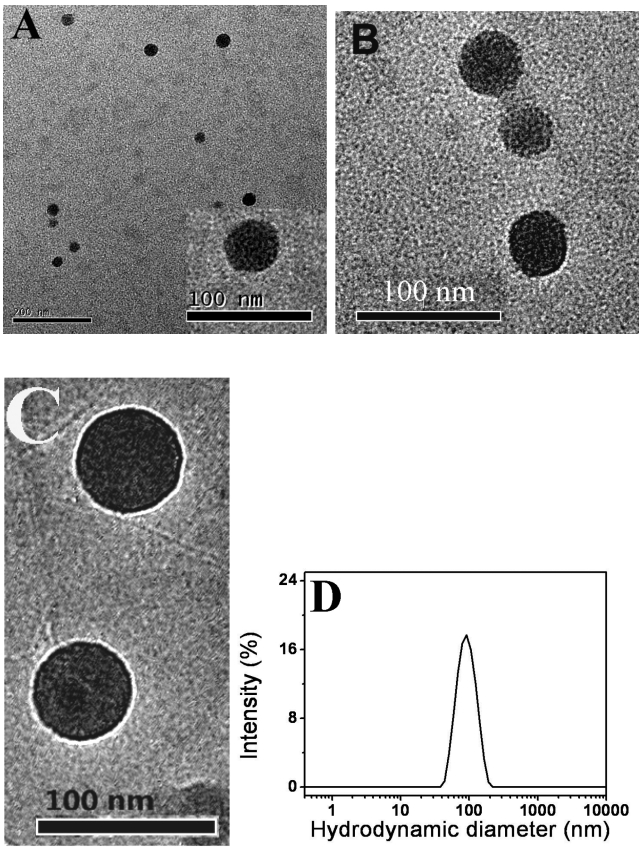

Figure 2. (A, B) TEM images of micelles self-assembled by PCL_{49}-b-PS_{227}-b-$POEGMA_9$ triblock terpolymer in an aqueous solution. The dark phases in the cores represent PS phases stained by RuO_4. (C) TEM image of the micelles on graphene oxide sheets. (D) Size distribution of triblock terpolymer micelles in aqueous solution determined by dynamic light scattering.

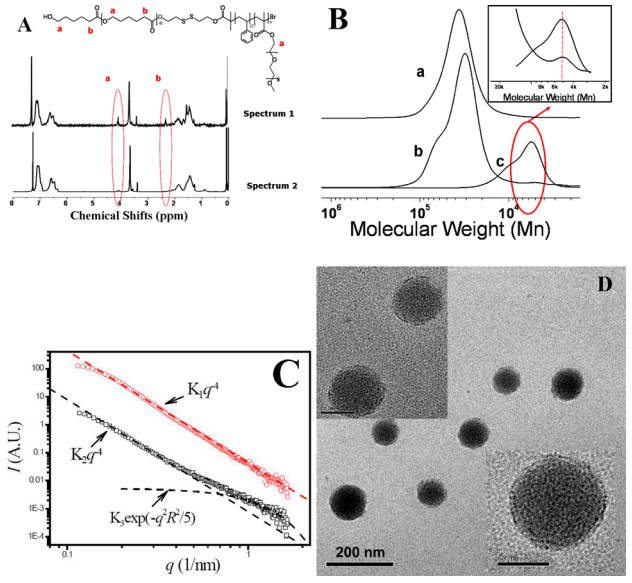

Figure 3. (A) ^1H NMR spectra of triblock terpolymer before (spectrum 1) and after (spectrum 2) PCL etching. (B) SEC traces of triblock terpolymer, PCL_{49}-b-PS_{227}-b-$POEGMA_9$, before (curve a) and after (curve b) PCL etching and precursor PCL homopolymer (curve c). (C) Small-angle X-ray scattering results of micelles self-assembled by PCL_{49}-b-PS_{227}-b-$POEGMA_9$ before (red circles) and after (black circles) PCL etching. (D) TEM images of micelles self-assembled by PCL_{49}-b-PS_{227}-b-$POEGMA_9$ after PCL etching. Insets show magnified images (scale bar = 50 nm).

distinct PCL and PS domains in the cores are created in acetonitrile (Figure S7, Supporting Information).

The solvated PCL blocks tethered to the core via disulfide bonds are chosen as the chemically etchable blocks, and the continuous PS phase forms the porous micellar core after PCL etching. To remove the PCL blocks from the micellar cores, excessive Bu_3P was added into the micellar solution under an argon atmosphere. After the cleavage reaction, aggregates were separated from the solution by centrifugation. Complete PCL removal was demonstrated by ^1H NMR. In the ^1H NMR spectrum, the absence of the signals at 2.29−2.33 ppm corresponding to the PCL blocks indicates the cleavage of the disulfide bonds and the removal of PCL blocks from the aggregates (Figure 3a). To further demonstrate the cleavage of the disulfide bonds, the micelles after PCL etching were directly dissolved in THF without removal of the PCL blocks and measured by SEC. SEC curves of PCL_{49}-b-PS_{227}-b-$POEGMA_9$ triblock terpolymer, micelles after PCL etching, and the precursor PCL homopolymer are given in Figure 3b. In comparison to the precursor triblock terpolymer, the SEC curve of the micelles shifts to the low molecular weight part after cleavage reaction, indicating the cleavage of the triblock terpolymer. It is also noted that on the SEC curve of the micelles (curve b) a small peak representing elution of the etched PCL has almost the same molecular weight as the precursor PCL homopolymer (inset in Figure 3b), demonstrating that PCL blocks are etched from the self-assembled structures. On the SEC curve of the micelles, the appearance of a small shoulder with a double molecular weight as the main peak is attributed to the oxidation of the thiol terminal groups into disulfide bonds in the preparation of the samples.

Small-angle X-ray scattering (SAXS) was employed to determine the average pore size. As shown in Figure 3c, the scattering curve of the micelles before cleavage reaction exhibits a q^{-4} dependence, reflecting a sharp interface between micelles and the medium.[29,30] After PCL etching, a small bump at $q > 0.4$ nm^{-1} shows up, which makes the scattering cure deviate from the q^{-4} dependence. The bump is related to the formation of the pores in the micellar cores.[26] On the basis of the scattering intensity function for monosized spheres,[30] the bump was fitted, and the average radius of the nanopores was calculated to be about 2.2 nm. TEM results indicate that micelles with porous cores are produced after PCL etching, and the average size of the pores is about 3 nm (Figure 3d). Because of the stabilization of POEGMA in the coronae, the micelles with porous cores do not aggregate together.

Ellman's reagent has been used widely for the quantitation of thiols in peptides and proteins.[31] However, in this research the concentration of the thiol group in the micellar solution is so low that the concentration can not be determined quantitatively by Ellman's reagent. To determine the amount of thiol groups in the pores, a small molecular compound with a disulfide group and two pyrenyl groups (Figure S8, Supporting Information) was used, and the amount of thiols in the micellar cores was determined by fluorescence analysis. Thiols inside the pores are able to have a thio−disulfide reaction with the compound,[32] and pyrenyl groups are tethered to the walls of the pores. On the basis of a standard curve made by the free compound dissolved in solutions, the concentration of pyrenyl groups inside the pores was determined by fluorescence

dx.doi.org/10.1021/mz400286d | ACS Macro Lett. 2013, 2, 891−895

analysis. Our calculation results show that in a milligram of polymeric micelles there are about 5.6×10^{-8} mol thiol groups, which means about 94% disulfide bonds inside the micellar cores were cleaved in the cleavage reaction of the triblock terpolymer. The standard curve and the emission spectrum of the micelles after grafting of pyrenyl groups to the pores are given in Figure S8 (Supporting Information).

The thiol groups in the pores are able to undergo many different chemical reactions, such as oxidation reaction and thiol−ene reaction. Attempts to modify the pore structures with functional groups were made in this research. FMA is a widely used fluorescent dye with a methacrylate group, which can conduct thiol−ene reaction with thiol groups under mild conditions.[25] After the reaction, polymeric micelles with FMA inside the pores were obtained. Photoluminescence (PL) results indicate that FMA-modified micelles do not have fluorescent emissions in neutral or acid solutions but present a strong emission with a peak at 512 nm in a basic medium (Figure 4a). In neutral or acid environments, the dye molecules

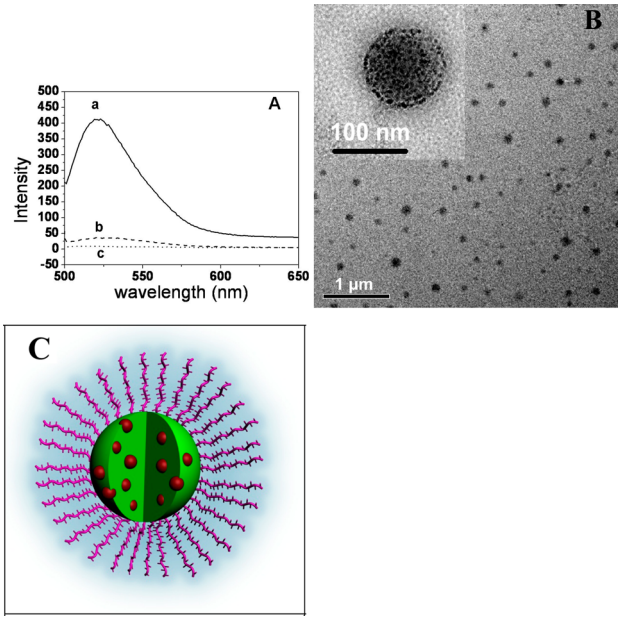

Figure 4. (A) Photoluminescence spectra of micelles decorated with FMA inside the pores in basic (curve a), acidic (curve b), and neutral (curve c) solutions. (B) TEM images of micelles with gold nanoparticles (AuNPs) inside pores. (C) Schematic depiction of the micelles with AuNPs prepared inside the pores.

are in the neutral form of fluorescein, so no emission was observed; however, in basic solution, the dye molecules are in the conjugated anionic form of fluorescein,[33] which present strong fluorescence emission. The fluorescence properties of FMA in the pores are very similar to the free FMA in aqueous solutions (Figure S9, Supporting Information).

The walls of the pores are decorated with active thiol groups, which are capable of providing facile access to the synthesis of well-defined hybrid materials. A typical example presented in this paper is the synthesis of AuNPs inside pores through thiol−gold interactions. For the preparation of AuNPs, the micelles were redispersed into an aqueous solution of $HAuCl_4$, and the entrapped gold ions in the pores were reduced by thiol groups without any external reducing agent.[34] As shown in the inset of Figure 4b, uniformly distributed AuNPs with sizes in the range of 2−3 nm are formed on polymeric micelles. The AuNPs are produced inside the pores, so the sizes of the AuNPs and their accommodations are very close. It is also noted that the morphology of the micelles is kept unchanged after loading of the AuNPs (Figure 4b). A schematic depiction of the hybrid micelles is presented in Figure 4c.

In conclusion, polymeric micelles with mesoporous cores were prepared by selective etching of the PCL discontinuous phases in the cores. After PCL etching, thiol groups were produced on the walls of the pores, and many different functional groups can be introduced to the micellar cores by thiol−ene or thio−disulfide reactions. Although modifications of the mesopores inside micellar cores with pyrenyl groups, FMA, and AuNPs were presented in this paper, similar nanoscopic structures should be accessible if different functional groups, especially some bioactive agents, are employed. Considering wide applications of polymeric micelles, controlled pore size, and the functional tunability of the structures, this strategy can find broad applications in the synthesis of new functional materials with fine structures.

■ ASSOCIATED CONTENT

Supporting Information

Experimental part, ^{1}H NMR, DLS curves, SEC curves, TEM images, and fluorescence spectra. This material is available free of charge via the Internet at http://pubs.acs.org.

■ AUTHOR INFORMATION

Corresponding Authors

*E-mail: nkliul@nankai.edu.cn.
*E-mail: hyzhao@nankai.edu.cn.

Notes

The authors declare no competing financial interest.

■ ACKNOWLEDGMENTS

This project was supported by the National Natural Science Foundation of China (NSFC) under contract 21074058, the National Basic Research Program of China (973 Program, 2012CB821500), and PCSIRT (IRT1257).

■ REFERENCES

(1) Tang, C.; Lennon, E. M.; Fredrickson, G. H.; Kramer, E. J.; Hawker, C. J. *Science* **2008**, *322*, 429−432.
(2) Arora, H.; Du, P.; Tan, K. W.; Hyun, J. K.; Grazul, J.; Xin, H. L.; Muller, D. A.; Thompson, M. O.; Wiesner, U. *Science* **2010**, *330*, 214−219.
(3) Discher, D. E.; Eisenberg, A. *Science* **2002**, *297*, 967−973.
(4) Liu, X.; Kim, J.; Wu, J.; Eisenberg, A. *Macromolecules* **2005**, *38*, 6749−6751.
(5) Cui, H.; Chen, Z.; Zhong, S.; Wooley, K. L.; Pochan, D. J. *Science* **2007**, *317*, 647−650.
(6) Dupont, J.; Liu, G.; Niihara, K.; Kimoto, R.; Jinnai, H. *Angew. Chem., Int. Ed.* **2009**, *48*, 6144−6147.
(7) Chen, Z.; Cui, H.; Hales, K.; Li, Z.; Qi, K.; Pochan, D. J.; Wooley, K. L. *J. Am. Chem. Soc.* **2005**, *127*, 8592−8593.
(8) Zhao, H.; Douglas, E. P.; Harrison, B. S.; Schanze, K. S. *Langmuir* **2001**, *17*, 8428−8433.
(9) Park, M.; Harrison, C.; Chaikin, P. M.; Register, R. A.; Adamson, D. H. *Science* **1997**, *276*, 1401−1404.
(10) Yoo, J. W.; Chambers, E.; Mitragotri, S. *Curr. Pharm. Des.* **2010**, *16*, 2298−2307.
(11) Rodriguez-Hernandez, J.; Checot, F.; Gnanou, Y.; Lecommandoux, S. *Prog. Polym. Sci.* **2005**, *30*, 691−724.

(12) O'Reilly, R. K.; Hawker, C. J.; Wooley, K. L. *Chem. Soc. Rev.* **2006**, *35*, 1068−1083.
(13) Jin, J.; Zhang, M.; Xiong, Q.; Sun, P.; Zhao, H. *Soft Matter* **2012**, *8*, 11809−11816.
(14) Jin, J.; Wu, D.; Sun, P.; Liu, L.; Zhao, H. *Macromolecules* **2011**, *44*, 2016−2024.
(15) Ringsdorf, H.; Schlarb, B.; Venzmer, J. *Angew. Chem., Int. Ed.* **1988**, *27*, 113−158.
(16) Li, Z.; Kesselman, E.; Talmon, Y.; Hillmyer, M. A.; Lodge, T. P. *Science* **2004**, *306*, 98−101.
(17) Moughton, A. O.; Hillmyer, M. A.; Lodge, T. P. *Macromolecules* **2012**, *45*, 2−19.
(18) Kubowicz, S.; Baussard, J. F.; Lutz, J. F.; Thuenemann, A. F.; von Berlepsch, H.; Laschewsky, A. *Angew. Chem., Int. Ed.* **2005**, *44*, 5262−5265.
(19) Li, Z.; Hillmyer, M. A.; Lodge, T. P. *Macromolecules* **2006**, *39*, 765−771.
(20) Marsat, J. N.; Heydenreich, M.; Kleinpeter, E.; von Berlepsch, H.; Böttcher, C.; Laschewsky, A. *Macromolecules* **2011**, *44*, 2092−2105.
(21) Seo, M.; Hillmyer, M. A. *Science* **2012**, *336*, 1422−1425.
(22) Trewyn, B. G.; Nieweg, J. A.; Zhao, Y.; Lin, V. S. Y. *Chem. Eng. J.* **2008**, *137*, 23−29.
(23) Heikkila, T.; Salonen, J.; Tuura, J.; Hamdy, M. S.; Mul, G.; Kumar, N.; Salmi, T.; Murzin, D. Yu.; Laitinen, L.; Kaukonen, A. M.; Hirvonen, J.; Lehto, V. P. *Int. J. Pharm.* **2007**, *331*, 133−138.
(24) Herman, J. J.; Jérome, R.; Teyssié, P. *Makromol. Chem.* **1981**, *182*, 997−1008.
(25) Lowe, A. B. *Polym. Chem.* **2010**, *1*, 17−36.
(26) Daniel, M. C.; Astruc, D. *Chem. Rev.* **2004**, *104*, 293−346.
(27) The number of PCL chains in a distinct domain can be calculated using the following equation

$$N = \frac{4}{3}\pi r^3 \rho \frac{N_A}{M_{PCL}}$$

where r is the average radius of the PCL domain measured by TEM; ρ is the density of PCL; M_{PCL} is the molecular weight of PCL; and N_A is Avogadaro's number.
(28) McHale, R.; Patterson, J. P.; Zetterlund, P. B.; O'Reilly, R. K. *Nature Chem.* **2012**, *4*, 491−497.
(29) Bock, V.; Emmerling, A.; Saliger, R.; Fricke, J. *J. Porous Mater.* **1997**, *4*, 287−294.
(30) Glatter, O.; Kratky, O., Eds. *Small-angle X-ray scattering*; Academic: London, 1982.
(31) Ellman, G. L. *Arch. Biochem. Biophys.* **1959**, *82*, 70−77.
(32) Singh, R.; Whitesides, G. M. *J. Am. Chem. Soc.* **1990**, *112*, 1190−1197.
(33) Nese, A.; Lebedeva, N. V.; Sherwood, G.; Averick, S.; Li, Y.; Gao, H.; Peteanu, L.; Sheiko, S. S.; Matyjaszewski, K. *Macromolecules* **2011**, *44*, 5905−5910.
(34) Negishi, Y.; Tsukuda, T. *J. Am. Chem. Soc.* **2003**, *125*, 4046−4047.